

Temperature-dependent surface structure, composition, and electronic properties of the clean SrTiO₃(111) crystal face: Low-energy-electron diffraction, Auger-electron spectroscopy, electron energy loss, and ultraviolet-photoelectron spectroscopy studies

Wei Jen Lo* and G. A. Somorjai

Materials and Molecular Research Division, Lawrence Berkeley Laboratory, and Department of Chemistry,
University of California, Berkeley, California 94720

(Received 23 December 1977)

Low-energy-electron diffraction, Auger-electron spectroscopy, electron-energy-loss, and ultraviolet-photoelectron spectroscopies were used to study the structure, composition, and electron energy distribution of a clean single-crystal (111) face of strontium titanate (perovskite). The dependence of the surface chemical composition on the temperature has been observed along with corresponding changes in the surface electronic properties. High-temperature Ar-ion bombardment causes an irreversible change in the surface structure, stoichiometry, and electron energy distribution. In contrast to the TiO₂ surface, there are always significant concentrations of Ti³⁺ in an annealed ordered SrTiO₃ (111) surface. This stable active Ti³⁺ monolayer on top of a substrate with large surface dipole potential makes SrTiO₃ superior to TiO₂ when used as a photoanode in the photoelectrochemical cell.

I. INTRODUCTION

Strontium titanate, SrTiO₃, is one of the few stable materials that can decompose water into hydrogen and oxygen with the assistance of light of band-gap energy 3.2 eV at 25 °C or greater in the photoelectrochemical cell.¹ The photoelectrolysis can be sustained using SrTiO₃ as an anode (where oxygen evolves) and platinum as a cathode (where hydrogen evolves), without the use of external potential. This may be contrasted with the TiO₂ photoanode² that requires +0.2 V external potential to carry out the same photoassisted water dissociation reaction in the same experimental configuration.

In addition to possessing this remarkable photocatalytic property, strontium titanate has interesting semiconducting, superconducting, and optical properties. Stoichiometric SrTiO₃ is an insulator transparent to visible light. At room temperature it is cubic but undergoes a transition to a tetragonal structure at about 110 K.³ When strontium titanate is reduced, it takes on a blue color and becomes semiconducting. Strontium titanate displays a number of interesting photochromic and electrochromic properties⁴ when doped with metal ions and hence has potentially important electro-optical applications in areas such as image storage, photochromism, and electrochromism. Doped strontium titanate is also a superconductor⁵ with a transition temperature of about 0.3 K. The atomic structure and electronic properties of bulk strontium titanate crystal have been thoroughly studied by theory and by experiments. Theoretical calculations of the bulk band structure of SrTiO₃ have

been reported by Kahn *et al.*⁶ and Matheiss⁷ and are in fairly good agreement with the results of photoemission experiments by Shirley *et al.*⁸ Compared to the data that have been accumulated on the bulk properties, the surface structure and electron energy distribution of the SrTiO₃ surface are relatively unexplored. Wolfram *et al.*⁹ have carried out surface-energy-band calculations of strontium titanate which suggests the existence of a highly localized *d*-electron surface band in the band-gap region and emphasizes its importance in surface chemical reactions. Experiments^{10,11} have been performed only recently that investigate the SrTiO₃ surface electron distribution, using ultraviolet-photoelectron spectroscopy (UPS).

Since the catalytic properties of surfaces depends strongly on their atomic surface structure, chemical composition, and electronic distribution, it is important to investigate all of these properties. In this report, a combination of surface-analysis techniques has been employed to characterize the clean strontium-titanate single-crystal face with (111) orientation. Low-energy-electron diffraction (LEED) and Auger-electron spectroscopy (AES) were used to study the surface structure and chemical composition, respectively. Electron energy distributions were studied by energy-loss spectroscopy (ELS) and UPS. It is found that for SrTiO₃, the crystal temperature plays an important role in determining its surface structure, chemical composition, and electronic distribution. By comparing the surface properties of TiO₂ and SrTiO₃, we attempt to explain the difference in the photoactivity observed when these materials were utilized in the photoelectrochemical cell.

II. EXPERIMENTAL

All the experiments were performed in a stainless-steel ultra-high-vacuum chamber evacuated by ion and water-cooled titanium sublimation pumps. The base pressure during these experiments was in the low 10^{-10} Torr range.

A double pass cylindrical mirror analyzer (CMA) with a coaxial electron gun was used as the primary electron source and electron energy analyzer by which electrons emitted into a conical segment with half angle of 42.3° from the axis of the analyzer were collected. In all Auger-electron analyses, the CMA was operated at a constant resolution of 1.5 eV. In this way we could resolve detail structures of the peaks in the dN/dE Auger spectra, and give reliable estimates of strontium to oxygen and oxygen to titanium ratios under different conditions of surface preparation.

A primary electron beam with energies between 60 and 180 eV was used in the electron-energy-loss experiments. The ELS were obtained either by directly measuring the electron energy distribution $N(E)$ as a function of energy loss or its second derivative $-d^2N/dE^2$. Both methods yielded the same loss peaks, except the features in the ELS $-d^2N/dE^2$ spectra were enhanced. The CMA was operated in the retarded mode with pass energy at 50 eV. Since the primary electron beam was not energy monochromatized, the ultimate resolution was limited by the thermal energy spread of the incident electrons which was about 0.5 eV. The energy positions of the loss peaks were independent of incident electron energies in the range of 60–180 eV. All energy-loss spectra reported in this paper were obtained with incident energies ~ 100 eV, whose features were very surface sensitive.

In the UPS studied, the cold cathode discharge lamp was operated to generate the He I spectral line at 21.2 eV. A self-made two-stage differential pumping manifold was employed to minimize the helium leak flow from the discharge lamp into the ultra-high-vacuum chamber which maintained a pressure of $1-2 \times 10^{-9}$ Torr during all UPS experiments. The mass spectrometer indicated that the pressure raise was due to the increase of helium partial pressure in the chamber. The specimen was positioned with its surface normal coincident with the axis of CMA. The angle of incidence of the photons on the specimen was 75° from the normal. The analysis was operated with a constant resolution of 0.35 eV. Typically, a spectrum could be obtained within 5 min.

The specimen used was a 99.99% undoped strontium-titanate single crystal with perovskite structure. Samples of (111) orientation, as determined

by the Laue back reflection technique, were cut from this crystal and mechanically polished using $0.05\text{-}\mu\text{m}$ Al_2O_3 powders. The specimen was then rinsed in distilled water and mounted on a high-density alumina holder, which had a tungsten heater wire located at the back of the sample to facilitate the radiation heating of the crystal. A LEED optics made by Physical Electronics was used to study the surface structure after annealing. Two samples of (111) orientation have been prepared and both gave essentially the same results.

For argon-ion bombardment of strontium-titanate surface, the vacuum chamber was back-filled with argon to a pressure of 6×10^{-5} Torr. With an accelerating voltage of 2 keV, the ion bombardment could typically deliver an argon-ion beam of $20 \mu\text{A}$ to the sample surface.

(a)



(b)



FIG. 1. Low-energy-electron-diffraction patterns of the clean SrTiO_3 (111) surface after Ar-ion bombardment at 27°C and subsequent annealing at 600°C . (a) $E_p = 24$ eV. (b) $E_p = 32$ eV.

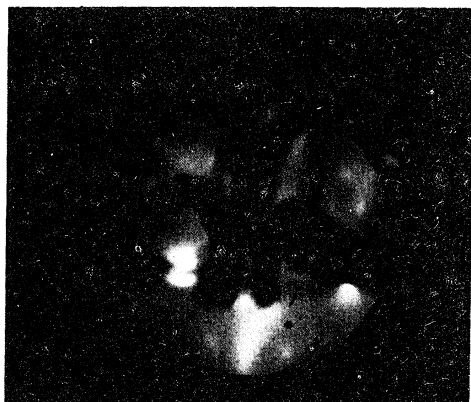
III. RESULTS

A. LEED and AES studies of the surface structure and chemical composition of clean SrTiO₃ (111) surface as a function of temperature

The LEED pattern obtained from the SrTiO₃ (111) surface at room temperature is shown in Fig. 1. The surface exhibits a stable 1×1 surface structure after Ar-ion bombardment at 27 °C to remove impurities then annealing at 600 °C for 30 min. However, after Ar-ion bombarding at 600 °C, the surface seems to facet as indicated by the LEED pattern (Fig. 2), and the surface assumes a complex structure. The 1×1 surface structure can be restored after removal of the faceted surface by extended Ar-ion bombardment (20 min) at 27 °C followed by annealing at 600 °C for 20 min.

The Auger-electron spectrum for the clean SrTiO₃ (111) 1×1 surface at 27 °C is shown in Fig.

(a)



(b)

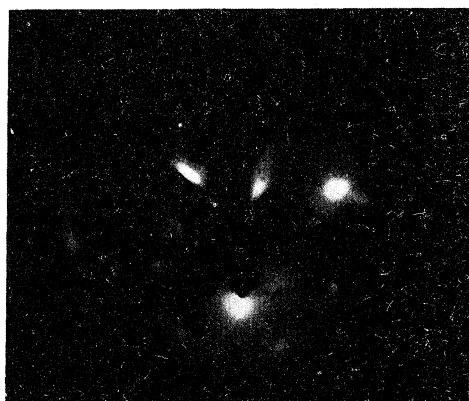


FIG. 2. Low-energy-electron-diffraction patterns of the clean SrTiO₃ (111) surface after Ar-ion bombardment at 600 °C and subsequent annealing at 600 °C. (a) $E_p = 25$ eV. (b) $E_p = 34$ eV.

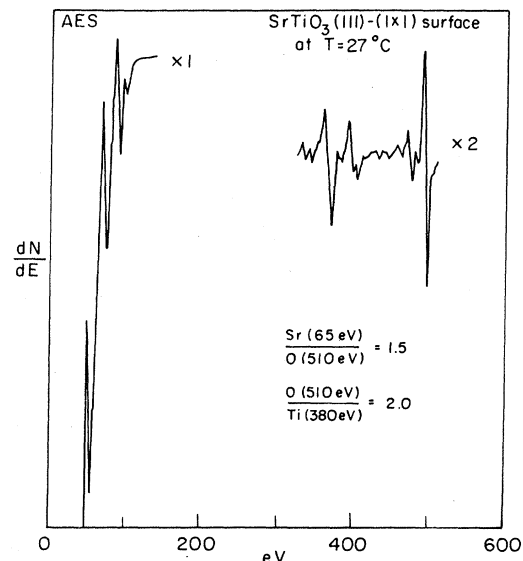


FIG. 3. Auger-electron spectrum of the clean ordered SrTiO₃ (111) 1×1 surface at 27 °C.

3. The value of the Auger peak-to-peak ratios of Sr (65 eV)/O (510 eV) and O (510 eV)/Ti (380 eV) in the AES spectrum for this surface are 1.5 and 2.0, respectively. Figure 4 shows the AES spectrum from the SrTiO₃ (111) surface at a temperature of 600 °C. By comparing with the AES spectrum in Fig. 3 we find the shape of titanium Auger peak at 416 eV has changed and the Auger Sr (65 eV)/O (510 eV) ratio drops to 1.1. The emission

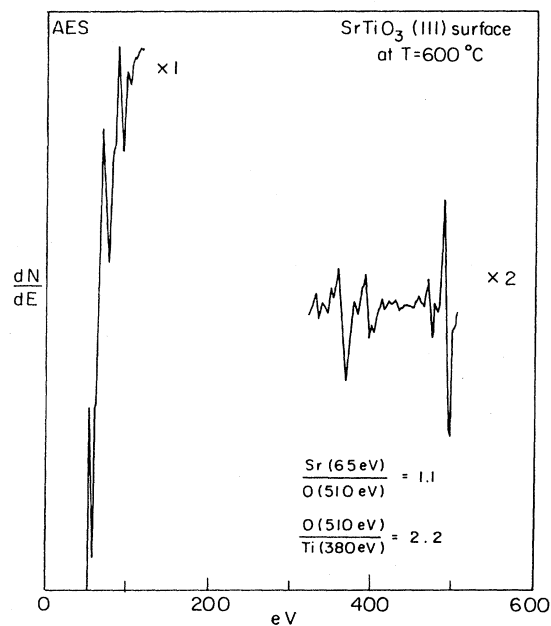


FIG. 4. Auger-electron spectrum of the clean ordered SrTiO₃ (111) surface at a temperature of 600 °C.

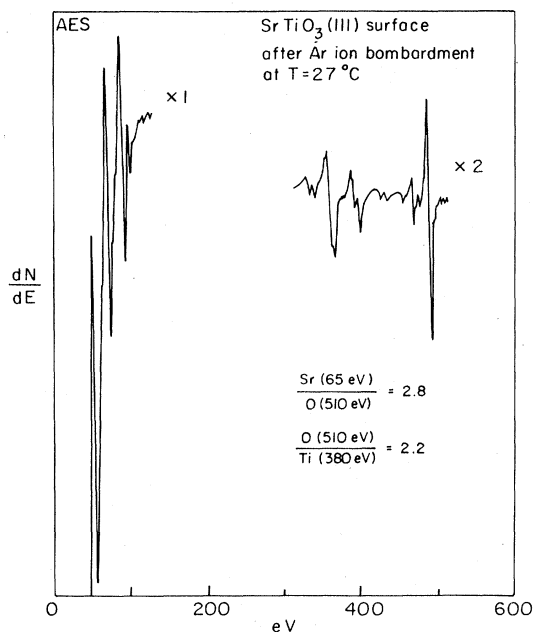


FIG. 5. Auger-electron spectrum of the clean room-temperature argon-ion-bombarded SrTiO₃ surface. The AES spectrum taken at 27 °C.

from the hot filament of the heater prevented LEED observation of SrTiO₃ (111) surface at 600 °C. After cooling the crystal to 27 °C, the AES spectrum returned to that shown in Fig. 3 and LEED showed a 1 × 1 surface structure at 27 °C. This heating and cooling cycle has been repeated several times and the above results are quite reproducible. It appears that the surface concentration of strontium becomes smaller with increasing temperature in a reversible manner.

Figure 5 shows the AES spectrum of the clean SrTiO₃ (111) surface after Ar-ion bombardment at 27 °C. The detailed feature of the Auger titanium and oxygen peaks in this AES spectrum are very similar to those of Ar-ion sputtered TiO₂ surface.¹² While there is only little change in the value of the Auger O (510 eV)/Ti (380 eV) ratio, upon ion bombardment, the Sr (65 eV)/O (510 eV) peak ratio shows a remarkable increase from 1.5 (for 1 × 1 surface) to 2.8 (for Ar-ion bombarded surface at 27 °C). It appears that Ar-ion bombardment at 27 °C removes oxygen preferentially from the surface region.

The AES spectra of the SrTiO₃ (111) surfaces which were Ar-ion bombarded at 27 and 600 °C, respectively, are shown in Fig. 6. Both spectra were taken at 27 °C after the same 2-keV Ar-ion dosage to the surface. Comparison of these spectra exhibits two distinct differences. First, we find that the shapes of titanium Auger peaks in the AES spectra are different. For the room-temper-

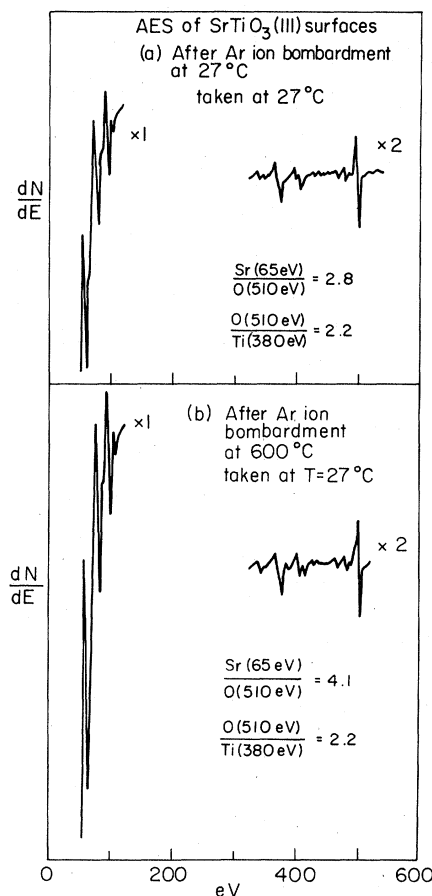


FIG. 6. AES spectra of: (a) room-temperature; (b) high-temperature (600 °C) Ar-ion-bombarded SrTiO₃ surfaces. Both spectra were taken at room temperature.

ature ion bombarded SrTiO₃ surface, the shape of the Auger titanium peak at 416 eV resembles that of the same peak in the Ar-ion sputtered TiO₂ surface. The shape of the corresponding titanium peak for the SrTiO₃ surface after Ar-ion sputtering at 600 °C resembles to that of the same peak in the well-annealed TiO₂ surface. Second, the value of the Auger Sr (65 eV)/O (510 eV) ratio is higher for the SrTiO₃ surface after high-temperature (600 °C) ion sputtering. It increases from 2.8 (for ion sputtering at 27 °C) to 4.1 (for ion sputtering at 600 °C). It appears that high-temperature argon-ion bombardment induces a large enrichment of strontium in the SrTiO₃ surface.

B. ELS and UPS studies of electron energy distribution at the clean SrTiO₃ (111) surface as a function of temperature

1. Electron-energy-loss spectroscopy

The ELS for the clean SrTiO₃ (111) crystal faces obtained after the different surface treatments are

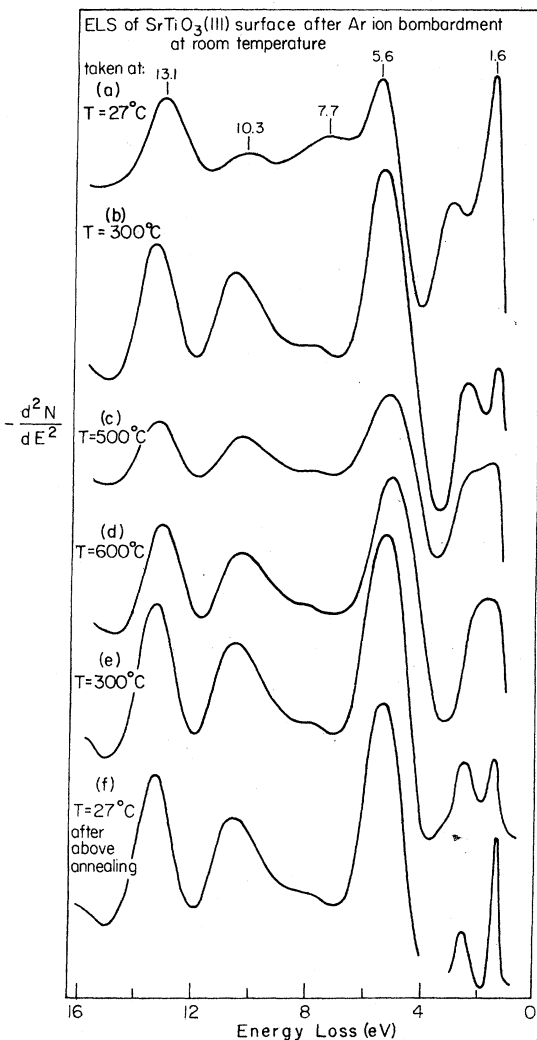


FIG. 7. ELS of the clean SrTiO_3 (111) surface at temperatures of (a) 27°C; (b) 300°C; (c) 500°C; (d) 600°C; (e) 300°C; (f) 27°C after room-temperature Ar-ion bombardment. The LEED pattern from the surface that corresponds to (f) indicates an ordered 1×1 surface structure.

shown in Fig. 7. In Fig. 7(a) the ELS spectrum of the clean SrTiO_3 surface is shown after Ar-ion bombardment at 27°C. There are six distinct transitions at 13.1, 10.3, 7.7, 5.6, 3.1, and 1.6 eV. The gross features of this spectrum are very similar to those reported for the Ar-ion sputtered TiO_2 surfaces,¹² except on the SrTiO_3 surface there is one more transition at 7.7 eV. Both TiO_2 and SrTiO_3 surfaces show a distinct 1.6-eV transition after Ar-ion sputtering at 27°C that is associated with the presence of Ti^{3+} ions at the surface.^{13,14} The ELS spectrum obtained at 300°C upon annealing the crystal at this temperature is shown in Fig. 7(b). The intensity of 10.3-eV transition has in-

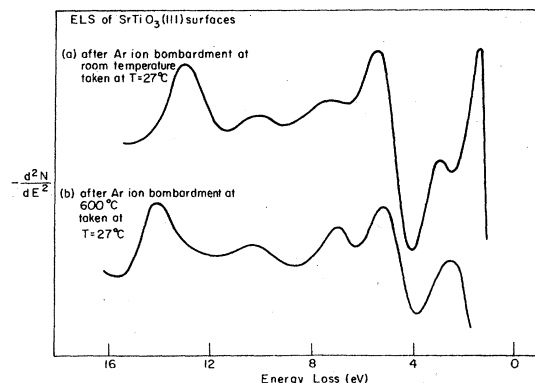


FIG. 8. ELS of the clean SrTiO_3 (111) surfaces (a) after room-temperature Ar-ion bombardment, (b) after high-temperature (600°C) Ar-ion bombardment. Both spectra were taken at room temperature of 27°C.

creased while the intensity of 7.7 eV has decreased. There is also an observable reduction in the intensity of the 1.6-eV transition. Figures 7(c) and 7(d) show the ELS spectra for the same SrTiO_3 crystal surface at 500 and 600°C, respectively. We find that there is a continuous reduction of the intensity of the 1.6-eV transition that is associated with the presence of Ti^{3+} and it finally disappears at 600°C. After cooling the crystal back to 300°C, the 1.6-eV transition reappears as shown in Fig. 7(e). Successive cooling of the crystal back to room temperature results in an ELS spectrum shown in Fig. 7(f). In comparison with that in Fig. 7(e), the intensity of 1.6-eV transition in Fig. 7(f) is enhanced. The surface LEED patterns that yield the ELS spectrum of Fig. 7(f) indicate the presence of an ordered 1×1 surface structure. The heating and cooling cycles have been repeated several times and the results are very reproducible. Thus, it appears that the composition and electronic energy distribution of the SrTiO_3 surface changes reversibly with surface temperature.

In Fig. 8, we show the ELS spectra for the SrTiO_3 surfaces that were Ar-ion bombarded at 27 and 600°C, respectively. Both surfaces have the same Ar-ion dosages and the spectra were obtained when the crystal reached room temperature after sputtering. Although the relative peak intensities of the 13.1-, 10.3-, 5.6-, and 3.1-eV transitions are similar in the two ELS spectra, the intensity of the 7.7-eV transition is higher in Fig. 8(b). In addition, while there is a distinct 1.6-eV transition in the ELS spectrum for the SrTiO_3 surface after Ar-ion bombardment at 27°C, this transition completely disappears from the ELS spectrum for the SrTiO_3 surface after high-temperature (600°C) Ar-ion sputtering.

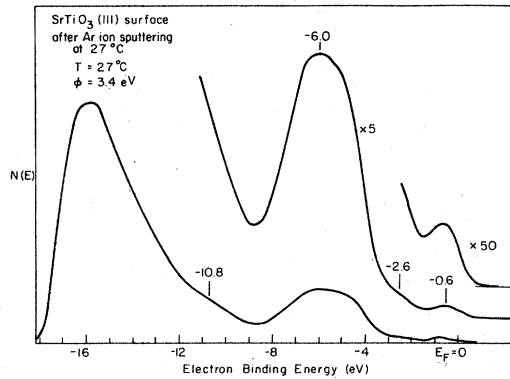


FIG. 9. UPS spectrum of the Ar-ion bombarded clean SrTiO_3 surface at 27°C .

2. Ultraviolet-photoelectron spectroscopy

The UPS spectrum for the Ar-ion sputtered surface at 27°C is shown in Fig. 9. In agreement with the work of Henrich,¹¹ an emission at -0.6 eV below the Fermi level E_F in the band-gap region is observed. This is consistent with the result obtained for Ar-ion bombarded TiO_2 surfaces,^{12,13} which show the same -0.6 eV emission in the UPS spectra. This emission is associated with the presence of Ti^{3+} in the oxide surfaces.^{13,14} In Fig. 9, there are also emission peaks with energies at -2.6 , -6.0 , and -10.8 eV, respectively. The work function ϕ of this surface is 3.4 eV.

Subsequent annealing at 600°C resulted in the disappearance of the -10.8 - and -2.6 -eV emissions and splitting of the broad -6.0 -eV peak into two emissions with energies at -6.9 and -4.8 eV, respectively, as shown in Fig. 10. We also find that the intensity of the -0.6 -eV emission in the band-gap region has been reduced. However, this emission always has a detectable intensity at 27°C , even after annealing the crystal at 800°C for

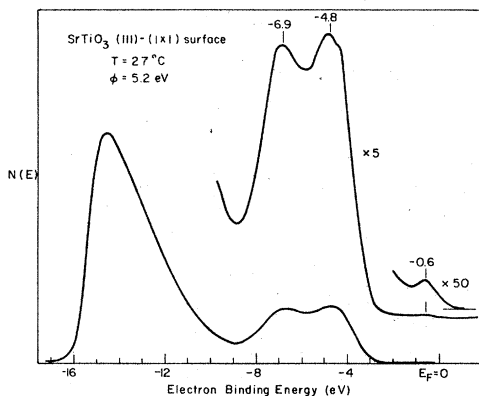


FIG. 10. UPS spectrum of the clean ordered SrTiO_3 (111) 1×1 surface. The spectrum was taken at a temperature of 27°C .

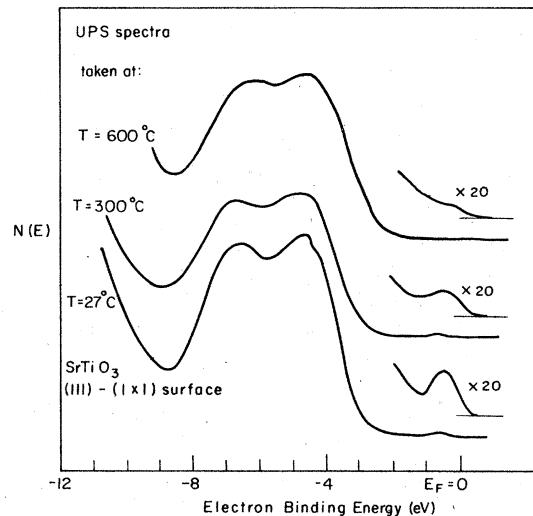


FIG. 11. UPS spectra of the clean ordered SrTiO_3 (111) surfaces taken at temperatures of 27 , 300 , and 600°C , respectively.

2 h. The LEED pattern which corresponds to the UPS spectrum shown in Fig. 10 indicates that the surface has a 1×1 structure. The work function of this clean ordered SrTiO_3 (111) 1×1 surface is 5.2 eV.

The temperature-dependent changes in the UPS spectra for the clean, ordered SrTiO_3 (111) surfaces are shown in Fig. 11 that displays the curves taken at 27 , 300 , and 600°C . There is a continuous reduction in the intensity of the -0.6 -eV emission with increasing crystal temperature. This change is reversible; after cooling the SrTiO_3 crystal to room temperature, the same initial UPS spectrum is obtained.

Figure 12 shows the UPS spectrum from the clean SrTiO_3 (111) surface after Ar-ion bombardment at 600°C . This spectrum was taken at a

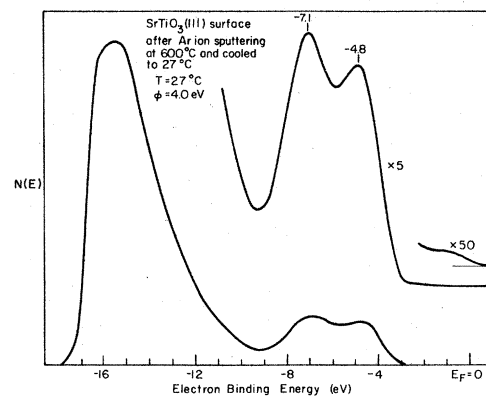


FIG. 12. UPS spectrum of the high-temperature (600°C) Ar-ion sputtered SrTiO_3 (111) surface. The spectrum was taken at 27°C .

crystal temperature of 27 °C after the high-temperature sputtering process. In contrast to the room-temperature Ar-ion-bombarded SrTiO₃ surface, we find that the Fermi-edge emission at -0.6 eV has disappeared almost completely. The work function of this surface is 4.0 eV.

IV. DISCUSSION

The change in the strontium-to-oxygen Auger peak ratio and the constancy of the oxygen-to-titanium ratio indicate oxygen and titanium are removed preferentially from the SrTiO₃ (111) surface by Ar-ion sputtering at room temperature. On annealing this sputtered surface, strontium diffuses into the bulk, thereby decreasing the strontium concentration of the surface. The chemical composition of the SrTiO₃ (111) surface can be varied reversibly by changing the crystal temperature as shown by AES. Although similar temperature-dependent surface composition has been observed for binary-alloy surfaces,¹⁵ our result is the first report of this effect for a ternary oxide compound.

Auger-electron spectroscopy analysis also shows that the crystal temperature during Ar-ion sputtering can cause marked changes in the chemical composition of the SrTiO₃ (111) surface. After a high-temperature (600 °C) Ar-ion sputtering treatment, there is a remarkable increase in the strontium concentration and annealing does not alter this surface composition any more. The room-temperature Ar-ion-bombarded SrTiO₃ surface has a lower strontium surface concentration and its value is decreased after annealing at 600 °C. This indicates that high-temperature Ar-ion bombardment yields a stable Sr-rich phase on the SrTiO₃ (111) surface, which behaves differently from the room temperature Ar-ion sputtered SrTiO₃ surface. Low-energy-electron diffraction studies also indicate structural differences between the two surfaces that were ion bombarded at 27 and 600 °C, respectively, after annealing.

The electron energy distributions of the SrTiO₃ (111) surface as a function surface treatments are studied by ELS and UPS. The transition peaks at 13.1, 10.3, 7.7, and 5.5 eV in the ELS spectra have also been observed by Cordova,¹⁶ using the ultraviolet reflectance technique. The bulk states which are involved in these transitions can be assigned.¹⁶ The ultraviolet-photoemitted electrons from the SrTiO₃ surface come from two sources: from the states in the valence band and from states in the band-gap region. While AES shows oxygen loss from the SrTiO₃ surface as a result of argon ion sputtering at 27 °C, the ELS spectrum of the Ar-ion sputtered SrTiO₃ surfaces shows a strong

peak at 1.6 eV. Since the band gap of SrTiO₃ is 3.2 eV, the initial states of the 1.6-eV transition must be located in the band-gap region. Indeed a band-gap emission at -0.6 eV in the UPS spectrum was found in this sputtered SrTiO₃ surface and was assigned to be the initial states for the 1.6-eV transition. Consistent with the results for the TiO₂ surfaces,¹²⁻¹⁴ these 1.6-eV transition and -0.6-eV emission are characteristic of the presence of surface Ti³⁺ species. In contrast to the case of the TiO₂ surface, where annealing caused the complete disappearance of Ti³⁺ species, the SrTiO₃ (111) 1 × 1 ordered surface after annealing always has detectable amounts of Ti³⁺ present at room temperature. The UPS spectrum of SrTiO₃ (111) 1 × 1 shows that the width of the valence band is 6.5 eV and two major emission peaks separated by 2.1 eV are resolved. This result is consistent with the recent x-ray photoelectron spectroscopy studies of Shirley *et al.*,⁸ and gives a reasonable fit to the density of states calculations of Mattheiss.⁷ The difference in the shapes of valence bands in the UPS spectra between the room-temperature Ar-ion sputtered SrTiO₃ surface and the SrTiO₃ (111) 1 × 1 surface is due to the change in surface stoichiometry that is induced by Ar-ion sputtering. In addition, the UPS spectrum of the SrTiO₃ surface after Ar-ion sputtering at 27 °C shows the presence of occupied states with energies around -2.6 eV which are located right above the valence-band maximum. The absence of these states on the SrTiO₃ (111) 1 × 1 surface after annealing indicates that they are extrinsic surface states induced by Ar-ion sputtering at 27 °C.

The reversible variation of the intensity of the -0.6-eV UPS emission and 1.6-eV ELS transition of SrTiO₃ surface as a function of temperature reveals that the concentration of surface Ti³⁺ species depends on the crystal temperature. At 27 °C, there is a large concentration of Ti³⁺ species (~10¹⁴/cm²) on the ordered surface. Raising the crystal temperature to 300 °C, reduces the Ti³⁺ concentration and a complete disappearance of Ti³⁺ species is obtained by heating the crystal above 600 °C.

Subsequent cooling of the crystal to room temperature results in the reappearance of the surface Ti³⁺ species. The combination of our ELS, UPS, and AES studies indicates that the temperature of the ternary oxide crystal controls its surface stoichiometry which in turn determines many of the surface electronic properties. The persistent difference in the surface Ti³⁺ species concentration between the TiO₂ and SrTiO₃ surfaces at room temperature indicates that excess Sr stabilizes the formation of Ti³⁺.

The combination of ELS, UPS, AES, and LEED

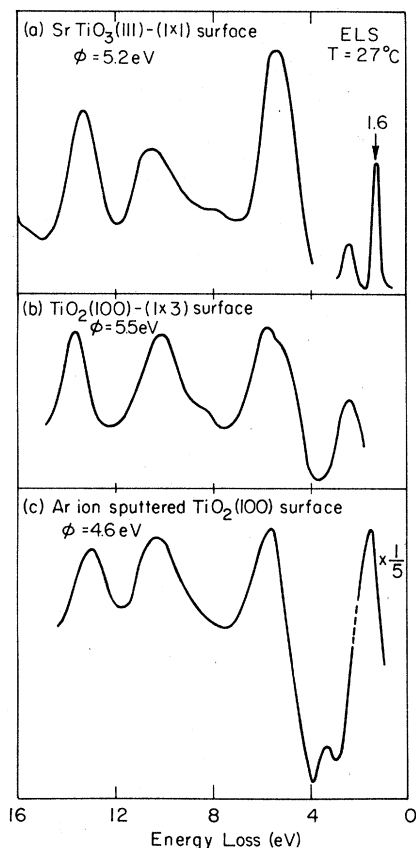


FIG. 3. ELS and the corresponding work functions of (a) clean ordered SrTiO₃ (111) 1×1 surface; (b) ordered TiO₂ (100) 1×3 surface; and (c) the clean Ar-ion sputtered TiO₂ surface. Note the persistent appearance of 1.6-eV transition on the SrTiO₃ (111) 1×1 surface which has also a larger work function than that of the Ar sputtered TiO₂ surface. All ELS spectra were taken at room temperature.

studies indicates that high-temperature (600 °C) Ar-ion sputtering treatment causes an irreversible change in the surface structure, surface chemical composition and electronic properties and yields a stable strontium-rich phase.

The different surface treatments of the SrTiO₃ surface result in drastic change of the work function and hence a large change in the surface dipole potential. In photoassisted reactions on the semiconductor surface where the transport of photo-

generated charge carriers at the surface is the rate-determining step, it is desirable to increase the electric field near the surface to allow a rapid charge transfer to and from the surface. In the case of TiO₂, Ar-ion sputtering produces a large concentration of Ti³⁺ species and a marked decrease in the surface dipole potential. Subsequent annealing increases the work function and the associated surface dipole potential, but removes all the Ti³⁺ species on the surface. However, in the case of SrTiO₃ surface where annealing also causes the increase of the work function, Ti³⁺ ions are always present at room temperature after annealing. Since the presence of surface Ti³⁺ species aids the dissociation of adsorbed water,¹³ an active Ti³⁺ monolayer on top of a substrate with large surface dipole potential provides a suitable catalyst for this photo-assisted reaction. The important differences in surface composition and work function shown in Fig. 13 appear to be the cause of the differences in photoactivity between TiO₂ and SrTiO₃ that are used in the photoelectrochemical cell.^{1,2}

V. CONCLUSION

Using LEED, AES, ELS, and UPS we have characterized the surface structure, composition, and electronic distribution of the (111) single-crystal surface of SrTiO₃. The dependence of the surface chemical composition on the temperature has been observed along with corresponding changes in the surface electronic properties. High-temperature Ar-ion bombardment causes an irreversible change in the surface structure, stoichiometry, and associated electron energy distribution. In contrast to the TiO₂ surface, there are always significant concentration of Ti³⁺ species on the SrTiO₃ surface, which also has a larger surface dipole potential. The stable, active Ti³⁺ monolayer on top of a substrate with large surface dipole potential makes SrTiO₃ superior to TiO₂ when used as a photoanode in the photoelectrochemical cell.

ACKNOWLEDGMENTS

We are grateful to V. E. Henrich for communicating his results to us prior to publication of his work. This work was supported by the Division of Basic Energy Sciences, U.S. Department of Energy.

*Also associated with Dept. of Physics, University of California, Berkeley, Calif. 94720.

¹(a) M. S. Wrighton, A. B. Ellis, P. T. Wolczanski, D. L. Morse, H. G. Abrahamson, and D. S. Grinley, *J. Am. Chem. Soc.* **98**, 2774 (1976); (b) M. S. Wrighton,

P. T. Wolczanski, and A. B. Ellis, *J. Solid State Chem.* **22**, 17 (1977).

²M. S. Wrighton, D. S. Gimley, P. T. Solczanski, A. B. Ellis, D. L. Morse, and A. Linz, *Proc. Natl. Acad. Sci. USA* **72**, 1518 (1975).

- ³Y. T. Sihvonen, *J. Appl. Phys.* **38**, 4431 (1967).
- ⁴B. Faughman, *Phys. Rev. B* **4**, 3623 (1971).
- ⁵J. F. Schooley, W. R. Hosler, E. Ambler, J. H. Becker, M. L. Cohen, and O. S. Koonce, *Phys. Rev. Lett.* **14**, 305 (1965).
- ⁶A. H. Kahn and A. J. Leyendecker, *Phys. Rev.* **135**, A1321 (1964).
- ⁷L. F. Mattheiss, *Phys. Rev. B* **6**, 4718 (1972).
- ⁸S. P. Kowalczyk, F. R. McFeely, L. Ley, V. T. Gritsyna, and D. A. Shirely, *Solid State Commun.* **23**, 161 (1977).
- ⁹T. Wolfram and F. J. Morin, *Appl. Phys.* **8**, 125 (1975).
- ¹⁰R. A. Powell and W. E. Spicer, *Phys. Rev. B* **13**, 2601 (1976).
- ¹¹J. G. Mavroides, V. E. Henrich, H. J. Zeiger, G. Dresselhaus, J. A. Kafalas, and D. F. Kolesar, *J. Electrochem. Soc.* (to be published).
- ¹²Y. W. Chung, W. J. Lo, and G. A. Somorjai, *Surf. Sci.* **64**, 588 (1977).
- ¹³W. J. Lo, Y. W. Chung, and G. A. Somorjai, *Surf. Sci.* **71**, 199 (1978).
- ¹⁴V. E. Henrich, G. Dresselhaus, and H. J. Zeiger, *Phys. Rev. Lett.* **36**, 1335 (1976).
- ¹⁵Steven H. Overbury, Ph.D. thesis (University of California, Berkeley, 1976) (unpublished).
- ¹⁶M. Cardona, *Phys. Rev.* **140**, A651 (1965).

(a)

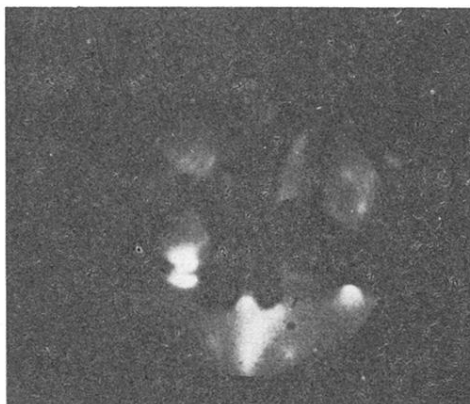


(b)



FIG. 1. Low-energy-electron-diffraction patterns of the clean SrTiO_3 (111) surface after Ar-ion bombardment at 27 °C and subsequent annealing at 600 °C. (a) $E_p = 24$ eV. (b) $E_p = 32$ eV.

(a)



(b)



FIG. 2. Low-energy-electron-diffraction patterns of the clean SrTiO_3 (111) surface after Ar-ion bombardment at 600°C and subsequent annealing at 600°C . (a) $E_p = 25$ eV. (b) $E_p = 34$ eV.